Farnesoid X Receptor Signaling Activates the Hepatic X-box Binding Protein 1 Pathway *in vitro* and in Mice

Xiaoying Liu[1], **Grace L. Guo**[2], **Bo Kong**[2], **David B. Hilburn**[1], **Susan C. Hubchak**[1], **Seong Park**[1], **Brian LeCuyer**[1], **Antony Hsieh**[1], **Li Wang**[3,4,5], **Deyu Fang**[6], and **Richard M. Green**[1]

[1]Division of Gastroenterology and Hepatology, Department of Medicine, Chicago, IL

[2]Department of Pharmacology and Toxicology, School of Pharmacy, Rutgers University, Piscataway, NJ

[3]Department of Physiology and Neurobiology, and the Institute for Systems Genomics, University of Connecticut, Storrs, CT

[4]Department of Internal Medicine, Section of Digestive Diseases, Yale University, New Haven, CT

[5]Veterans Affairs Connecticut Healthcare System, West Haven, CT

[6]Department of Pathology, Northwestern University Feinberg School of Medicine, Chicago, IL

Abstract

Bile acids are endogenous ligands of the nuclear receptor farnesoid X receptor (FXR), and pharmacologic FXR modulators are under development for the treatment of several liver disorders. The inositol-requiring enzyme 1α/X-box binding protein 1 (IRE1α/XBP1) pathway of the unfolded protein response (UPR) is a protective cellular signaling pathway activated in response to endoplasmic reticulum stress. We investigated the role of FXR signaling in the activation of the hepatic XBP1 pathway. Mice were treated with deoxycholic acid (DCA), cholestyramine, GW4064 or underwent bile duct ligation (BDL) and the hepatic UPR activation was measured. Huh7-Ntcp and HepG2 cells were treated with FXR agonists, inhibitor, siRNA or SHP siRNA to determine the mechanisms of IRE1α/XBP1 pathway activation. DCA feeding and BDL increased and cholestyramine decreased expression of hepatic XBP1s. XBP1 pathway activation increased in Huh7-Ntcp and HepG2 cells treated with bile acids, 6-ECDCA or GW4064. This effect decreased with FXR knockdown and treatment with FXR inhibitor guggulsterone. FXR agonists increased XBP1 splicing and phosphorylated-IRE1α expression. Overexpression of small heterodimer partner (SHP) similarly increased XBP1 splicing, XBP1s and phosphorylated-IRE1α protein expression. SHP knockdown attenuated FXR agonist-induced XBP1s and phosphorylated-IRE1α protein expression. Co-immunoprecipitation assays demonstrate a physical interaction between overexpressed GFP-SHP and FLAG-IRE1α in HEK293T cells. Mice treated with GW4064 had increased, and FXR and SHP null mice had decreased, basal *Xbp1s* gene expression.

To whom correspondence should be addressed: Richard M. Green, MD, Division of Gastroenterology and Hepatology, Department of Medicine, Northwestern University, Tarry 15-719, 303 E. Chicago Ave, Chicago, IL 60611; Phone: 312-503-1812; Fax: 312-908-9032; Rigreen@nm.org.

Author names in bold designate shared co-first authorship.

Conclusion—FXR signaling activates the IRE1α/XBP1 pathway *in vivo* and *in vitro*. FXR pathway activation increases XBP1 splicing and enhances phosphorylated-IRE1α expression. These effects are mediated, at least in part, by SHP. IRE1α/XBP1 pathway activation by bile acids and pharmacologic FXR agonists may be protective during liver injury and may have therapeutic implications for liver diseases.

Keywords

bile acid; obeticholic acid; IRE1α; SHP; unfolded protein response

The unfolded protein response (UPR) is an adaptive cellular response to endoplasmic reticulum (ER) stress that maintains homeostasis by increasing protein processing capacity and attenuating protein translation (1–3). The UPR is important in many hepatic diseases including cholestasis, non-alcoholic fatty liver disease, alpha-1 antitrypsin deficiency, ischemia-reperfusion injury and viral hepatitis (4). However, the cellular mechanisms regulating the hepatic UPR remain incompletely understood. Three UPR pathways are activated through the transmembrane ER sensors: inositol-requiring enzyme 1α (IRE1α), PKR-like ER kinase (PERK), and activating transcription factor 6 (ATF6); and the IRE1α/X-box binding protein 1 (XBP1) pathway is the evolutionarily most conserved. When ER stress occurs, IRE1α auto-phosphorylates and activates its endoribonuclease activity that is responsible for the unconventional splicing of XBP1 mRNA. IRE1α splices a 26-nucleotide sequence from unspliced XBP1 (XBP1u) mRNA and causes a translational frameshift, producing the transcriptionally active XBP1 spliced (XBP1s). XBP1s regulates downstream target genes such as ERdj4 to promote protein folding and ER-associated degradation (ERAD) (5, 6). This pathway has been implicated in the pathogenesis, and as a protective response, in several forms of liver injury (7–9). *In vitro* studies demonstrate that the bile acid deoxycholic acid (DCA) causes protein unfolding and aggregation (10). However, the molecular mechanisms by which cholestasis or bile acid signaling regulates the XBP1 pathway remain unexplored.

Bile acids are endogenous ligands of the nuclear receptor farnesoid X receptor (FXR) and activation of hepatic FXR regulates the expression of many genes in the liver (11, 12). Many inhibitory effects on gene expression are due to FXR-mediated induction of small heterodimer partner (SHP), which is considered a universal transcriptional inhibitor (13). There is also SHP-independent gene regulation by direct transcriptional activation of FXR target genes (11, 12, 14, 15). FXR plays important roles in maintaining bile acid homeostasis, as well as regulating lipid and cholesterol metabolism (15, 16). Pharmacologic FXR agonists are therapeutic in several experimental models of liver injury and are currently approved or in clinical trials for metabolic and cholestatic liver diseases. Interactions of the FXR pathway and the hepatic UPR, however, remain unexplored. The purpose of this study is to determine the role of bile acid and FXR signaling in the regulation of the hepatic IRE1α/XBP1 pathway. These studies will enhance our understanding of the role of the UPR in liver diseases and may have important therapeutic implication.

Experimental Procedures

Material

Bile acids and cholestyramine were purchased from Sigma-Aldrich (St. Louis, MO). GW4064, (z)-guggulsterone and 6-ECDCA (obeticholic acid) were purchased from Cayman Chemical (Ann Arbor, MI). FXR, SHP siRNA and scramble siRNA were purchased from GE Dharmacon (Lafayette, CO). Lipofectamine® RNAiMax and LTX transfection reagents were purchased from ThermoFisher (Waltham, MA). Antibodies against XBP1 and GAPDH were from Proteintech (Chicago, IL), β-actin, FLAG and GFP antibodies were from Sigma-Aldrich (St. Louis, MO), IRE1α antibody was from Cell Signaling Technology (Danvers, MA) and phosphorylated-IRE1α antibody was from Novus Biologicals (Littleton, CO). SHP antibody was from Santa Cruz Biotechnology (Dallas, TX).

Animal Experimentation

FVB/NJ, C57BL/6J and FXR (−/−) mice (8-10 weeks) were purchased from Jackson Laboratory (Bar Harbor, ME). SHP (−/−) mice colonies were maintained as previously reported (17). Mice were maintained under 12-hour light/dark cycles with unlimited access to regular chow and water until the first day of the study. For feeding experiments, male FVB/NJ mice received chow, chow supplemented with 0.3% (w/w) deoxycholic acid (DCA) or chow supplemented with 2% (w/w) cholestyramine for up to 7 days. Male C57BL/6J mice were gavaged with GW4064 (150 mg/kg) as previously described (18). At the conclusion of each experiment, mice were fasted for 4 hours, the livers were excised, flash-frozen in liquid nitrogen and stored at −70°C. Whole blood was obtained from the right atrium by cardiac puncture. For mice used in bile acid analysis, the liver, gallbladder and small intestine were collected and minced in 100% methanol. Bile duct ligation in female C57BL/6J mice was performed by the Northwestern University Microsurgery Core. All protocols and procedures were approved by the Northwestern University Institutional Animal Care and Use Committee guidelines.

Serum Alanine Aminotransferase (ALT) Assay

Serum ALT was measured using a spectrophotometric assay according to the manufacturer's protocol (Teco Diagnostics, Anaheim, CA).

Analysis of Bile Acid Pools

Total bile acid pool size and composition were measured by high-performance liquid chromatography as previously described (19). Samples were spiked with glycocholic acid as an internal standard to control for extraction efficiency. Individual bile salt species were identified by their characteristic retention times and by using bile acid standards.

Cell Culture and siRNA Transfection

HepG2 cells (ATCC, Manassas, VA) were cultured in EMEM with 10% fetal bovine serum (FBS) and maintained at 37°C in 5% CO_2. Lenti-X™ HEK293T cells (Takara Bio., Mountain View, CA) were cultured in DMEM with 10% FBS and 4 mM glutamine. Huh7 cells stably expressing rat sodium-taurocholate polypeptide (Huh7-Ntcp) were kindly

provided by Dr. Simon Hohenester (University of Munich, Munich, Germany) and were grown in minimal essential medium containing 10% FBS, 1% nonessential amino acids, 2 mM-glutamine, 1 mM sodium pyruvate, 100 units/ml penicillin, 100 μg/ml streptomycin, and 0.25 μg/ml amphotericin B (20). Cells were grown to 80% confluence and serum-deprived for 24 hours before treatment with TCA, TDCA, TCDCA, 6-ECDCA, GW4064 or vehicle. In guggulsterone studies, cells were pretreated with 50 μM guggulsterone for 1 hour prior to receiving either DMSO or 6-ECDCA. For siRNA transfection studies, HepG2 cells were transfected with 7.5 pmol of FXR siRNA, 9.5 pmol of SHP or scramble siRNA using Lipofectamine® RNAiMax for 48 hours prior to GW4064 treatment according to the manufacturer's protocol.

Luciferase Reporter Assay

The XBP1-luc reporter vector was kindly provided by Dr. Albert Koong (Stanford University, Palo Alto, CA) to assay the atypical splicing of the XBP1 mRNA (21). Huh7-Ntcp or HepG2 cells were transfected with 0.45 μg XBP1-luc reporter gene and 0.05 μg Pol III-Renilla luciferase vector as a control for transfection efficiency using Lipofectamine® LTX transfection reagent per manufacturer's instruction. After a 48-hour transfection, cells were treated with 6-ECDCA, GW4064 or DMSO for 8 hours. For SHP over-expression study, Huh7-Ntcp or HepG2 cells were co-transfected with a total of 2.0 μg of vector using pcDNA3 or human GFP-SHP (0-2.0 μg) expression plasmid (22) with or without 0.45 μg XBP1-luc reporter gene vector and 0.05 μg Pol III-Renilla luciferase vector for 48 hours. At the end of experiment, the cells were harvested in passive reporter lysis buffer. Firefly and Renilla luciferase activities were measured with a dual-luciferase reporter assay kit (Promega, Madison, WI). All experiments were performed in triplicate. The luciferase activity was calculated as the ratio of Firefly:Renilla luminescence.

RNA Extraction and Quantitative Real-Time Polymerase Chain Reaction (qPCR)

Total RNA was extracted from frozen liver or cell culture using TRIzol® reagent according to the manufacturer's protocol (ThermoFisher, Waltham, MA). qPCR was performed as described previously (7). All primers were synthesized by Integrated DNA Technology (Coralville, CA).

Co-immunoprecipitation

HEK293T cells were transfected with pcDNA3, human SHP-GFP or human FLAG-IRE1α (23) plasmids using Calfectin reagent (SignaGen Laboratories, Rockville, MD) according to the manufacturer's protocol. Forty-eight hours post transfection, cells were rinsed with cold PBS, scraped into tubes, centrifuged and pellets flash frozen in liquid nitrogen before -70ºC storage. For immunoprecipitation experiments, pellets were lysed in 150 mM NaCl, 20 mM Tris, 1 mM EDTA (NTEN) buffer containing protease and phosphatase inhibitors, cleared by centrifugation and protein concentration estimated. Lysates (750 μg) were precleared with Protein A/G beads then immunoprecipitated overnight, 4ºC, with 2 μg SHP or 1 μg FLAG antibodies. Immunoprecipitates were captured with Protein A/G beads, washed extensively with NTEN buffer, before elution by heating in 2x loading buffer. NTEN buffer alone was used as a negative control. Eluates and reserved lysate (input) were electrophoresed and transferred to PVDF membranes and probed with indicated antibodies.

Western Immunoblotting

Protein homogenates from frozen livers or cultured cells were isolated and used with western immunoblotting as described previously (7). Nuclei preparations were performed using nuclear extraction kit (Caymen Chemical, Ann Arbor, MI) according to the instructions of the manufacturer.

Statistics

Each experiment was repeated a minimum of three times. Data are shown as means ± SEM. Comparison between two groups was performed by Student's *t*-test. Statistical significance was defined as *P* values of less than 0.05.

Results

Deoxycholic acid feeding increases bile acid pool and hepatic XBP1 pathway expression

It has previously been reported that feeding cholic acid to mice increases hepatic *Xbp1s* expression, presumably due to the presence of ER stress (24). We hypothesized that *Xbp1s* induction may be mediated, at least in part, by FXR signaling activation of phosphorylated-IRE1α (p-IRE1α) with a resultant increase in hepatic XBP1s expression. We fed mice with a diet containing 0.3% deoxycholic acid (DCA) for 0, 1, 3 and 7 days to enrich the bile acid FXR ligands. As shown in Figure 1A, nuclear expression of XBP1s protein was increased after 1 and 3 days of DCA feeding. Hepatic nuclear XBP1s was not detectable at baseline or at 7 days. p-IRE1α was not detected at any time point due to low level of expression in wild-type mice. Figure 1B demonstrates that hepatic gene expression of *Xbp1s* and its downstream target *ERdj4* increased 6-fold and 1.5-fold, respectively in DCA-fed mice compared to chow-fed controls (*P* < 0.05). Figure 1C demonstrates that DCA feeding for one day resulted in a 2-fold increase in the total bile acid pool (*P* < 0.001), and significant increases in the FXR bile acid ligands taurochenodeoxycholic acid (TCDCA), taurocholic acid (TCA) and taurodeoxycholic acid (TDCA). TCDCA and TDCA contents were 1.2±0.3 and 1.8±0.6 μmol/100g mouse, respectively, in DCA-fed mice, while both bile acids were non-detectable in chow-fed mice (*P* < 0.05). TCA increased 7-fold in DCA fed mice, being 52.0±3.6 versus 7.3±1.6 μmol/100g mouse (*P* < 0.001). Serum ALT levels were similar in the mice fed chow or DCA for one day, and increased at day 3 and 7 (Supporting Figure S1); all liver histology was normal. Hepatic gene expression of the UPR genes *Atf4*, *Atf6*, *Bip* and *Chop* did not increase at any time points, and in fact, gene expression of *Atf4* and *Atf6* decreased at 7 days (Figure 1B). This suggests that bile acid feeding may activate the liver XBP1s pathway.

Bile duct ligation increases hepatic XBP1s expression

In order to determine if the IRE1α/XBP1 pathway is activated in another model of cholestasis, bile duct ligation (BDL) or sham laparotomy was performed on C57BL/6J mice for 48 hours. Serum ALT and alkaline phosphatase (ALP) were higher in the BDL group (ALT: 734±412 vs 28±3 U/L; ALP: 251±66 vs 83±6 U/L, *P* < 0.05 in BDL vs sham, respectively). Figure 1D demonstrates that 48 hours after BDL, hepatic *Xbp1s* mRNA

increased 4-fold ($P < 0.001$) and Figure 1E shows that XBP1s nuclear protein increased significantly.

Reducing bile acid pool with cholestyramine decreases hepatic XBP1 pathway expression

Since expansion of the bile acid pool with DCA feeding may potentially cause ER stress, we fed mice a diet containing 2% (w/w) cholestyramine for 7 days to reduce the bile acid pool, and measured the effect on liver IRE1α/XBP1 signaling. Figure 2 demonstrates that feeding cholestyramine for 7 days resulted in significant reductions of basal gene expression of *Xbp1s*, *Xbp1u* and *Ire1a* by 58%, 46% and 35%, respectively ($P < 0.05$); while basal *ERdj4* expression did not change. Baseline p-IRE1α and XBP1s protein levels were not detected. Hepatic gene expression of *Atf4, Atf6*, *Bip* and *Chop* was not diminished by cholestyramine feeding, and in fact, *Atf6* expression increased slightly at 7 days.

Bile acids activates IRE1α/XBP1 pathway *in vitro*

Since the hepatic XBP1 pathway was activated by expansion of the bile acid pool and in response to BDL, and basal gene expression of the XBP1 pathway was reduced by contraction of the bile acid pool, we next investigated the *in vitro* effects of bile acids on the XBP1 pathway. Initial experiments demonstrated that treating Huh7-Ntcp cells for 6 hours with 0-100 μM concentrations of TDCA, TCDCA and TCA increased XBP1s protein expression in a dose-dependent manner; with XBP1s protein expression increases evident at 10 μM bile acid concentration (Supporting Figure S2). Therefore, we treated Huh7-Ntcp cells for 6 hours with 10 μM of TDCA, TCDCA, TCA or vehicle and determined the effect on the XBP1 pathway. Gene expression of *XBP1s*, *ERdj4* and *IRE1a* all increased in response to treatment with each bile acid, and *SHP* expression increased 5 to 8-fold (Figure 3A). XBP1s protein expression similarly increased, with greater effects occurring in response to the FXR ligands TCDCA and TCA (Figure 3B). Therefore, the bile acid species that were enriched *in vivo* by DCA feeding also activate the IRE1α/XBP1 pathway *in vitro*.

FXR agonists activates IRE1α/XBP1 pathway *in vitro*

Since bile acids are endogenous ligands of the nuclear receptor FXR, we then treated Huh7-Ntcp cells and HepG2 cells with high affinity pharmacologic FXR agonists to determine the effects of FXR signaling on the XBP1 pathway. Figure 4A and 4B demonstrate that treating Huh7-Ntcp cells with the high affinity FXR agonist 6-ECDCA (0-10 μM) for 4 hours increased gene expression of *XBP1s*, *ERdj4* and *IRE1a*; as well as XBP1s protein expression in a dose-dependent manner. Figures 4C and 4D show that treating HepG2 cells with the FXR ligand GW4064 (0-2.5 μM) for 6 hours similarly increased both gene expression of *XBP1s*, *ERdj4* and *IRE1a*; and protein expression of XBP1s in a dose-dependent manner. No changes of XBP1s expression occurred within 2 hours of treatment in either cell type (Supporting Figure S3A, S3B). As expected, both FXR agonists increased gene expression of *SHP* (Figure 4A, 4C and Supporting Figure S3C, S3D).

FXR inhibition and knockdown decreases FXR agonists-activated XBP1s protein expression

We subsequently investigated the effects of the FXR inhibitor guggulsterone and FXR knockdown on both basal and FXR agonist-induced XBP1s protein expression. Huh7-Ntcp cells were treated with 10 μM 6-ECDCA or vehicle, in the presence or absence of 50 μM guggulsterone. Figure 5A demonstrates that both basal and 6-ECDCA-induced XBP1s protein expression were blocked by pre-treatment with guggulsterone. In fact, protein expression of XBP1s in 6-ECDCA and guggulsterone co-treated cells remained below the basal XBP1s expression levels of untreated controls. Since inhibitors may lack specificity, and to further confirm the inhibitory effect of guggulsterone, we used HepG2 cells transfected with FXR siRNA (or scramble siRNA) to demonstrate that FXR knockdown similarly decreased both basal and GW4064-induced increases in XBP1s protein expression (Figure 5B). Supporting Figure S4A confirms that FXR siRNA treatment reduced expression of *FXR* mRNA by over 70%.

FXR agonists induce XBP1 splicing and IRE1α phosphorylation

The atypical splicing of XBP1 into its active spliced form by IRE1α is a major regulatory mechanism for the IRE1α/XBP1 pathway (6, 25). We utilized an XBP1 splice activity luciferase-reporter gene construct (XBP1-luc) to measure the effect of FXR agonists on XBP1 splicing. Figure 6A demonstrates that treatment of Huh7-Ntcp and HepG2 cells with either 10 μM 6-ECDCA or 2.5 μM GW4064 for 8 hours increased XBP1 splicing compared to DMSO vehicle-treated cells (*P* < 0.01). DMSO-treated cells had identical luciferase activity to untreated cells.

The phosphorylated form of IRE1α (p-IRE1α) is the active form that splices *Xbp1u* into *Xbp1s*. Thus, we measured the expression of p-IRE1α in Huh7-Ntcp and HepG2 cells treated with 6-ECDCA and GW4064, respectively. Figure 6B shows the expression of p-IRE1α in Huh7-Ntcp cells increased as early as 2 hours after the administration of 6-ECDCA and Figure 6C shows p-IRE1α expression in HepG2 cells increased by 4 hours after treatment with GW4064. There were no increases in p-IRE1α expression at earlier time points in either cell types (Supporting Figure S3A, S3B). These data indicates that FXR agonist-induced XBP1s expression was associated with increases in both p-IRE1α expression and XBP1 splice activity. Of note, the gene expression of polo-like kinase 3 (PLK3) was not changed at 1 or 2 hours after 6-ECDCA or GW4064 treatment, indicating that increased p-IRE1α expression was not associated with *PLK3* gene induction.

SHP is associated with FXR agonist-induced activation of IRE1α/XBP1 pathway

Since many FXR signaling effects are mediated by SHP, and SHP mRNA expression was up-regulated as early as 30 minutes or 1 hour in GW4064-treated HepG2 cells or 6-ECDCA-treated Huh7-rNTCP cells, respectively (Supporting Figure S3C, S3D), we next overexpressed human SHP in HepG2 cells to determine the effect on the activation of IRE1α/XBP1 pathway. Figure 7A demonstrates a dose-response curve of transfections (0-2 μg) overexpressing SHP using a GFP-tagged SHP plasmid. SHP overexpression resulted in a dose-dependent increase of the XBP1-luc reporter luciferase activity, indicative of increased

splicing activity. Figure 7B further shows that this was associated with increased XBP1s and p-IRE1α protein expression.

To further confirm the specific role of SHP in IRE1α/XBP1 pathway activation, we performed SHP knockdown experiments using SHP siRNA. Figure 7C demonstrates that SHP knockdown decreased GW4064-induced XBP1s and p-IRE1α protein expression in HepG2 cells. Supporting Figure S4B confirms that SHP siRNA treatment reduced expression of *SHP* mRNA by 79%. These data suggest that FXR agonist-induced IRE1α/XBP1 pathway activation is, at least in part, mediated by SHP.

Although SHP acts as a transcriptional repressor localized primarily in the nucleus, SHP also localizes and interacts with proteins in other cellular compartments (26). SHP is highly expressed in microsome-enriched subcellular fraction (27). Since IRE1α is an ER resident protein, we investigated a potential interaction between SHP and IRE1α which may lead to the activation of the IRE1α/XBP1 pathway. SHP and IRE1α were overexpressed in HEK293T cells with GFP-SHP and FLAG-IRE1α plasmids. Co-immunoprecipitation experiments demonstrate a physical interaction between SHP and IRE1α using immunoprecipitation assays with a FLAG (Figure 7D) or SHP antibody (Figure 7E). These data suggest that SHP could possibly activate IRE1α/XBP1s through a non-transcriptional mechanism.

FXR/SHP signaling regulates hepatic XBP1 expression *in vivo*

In order to determine the *in vivo* effects of FXR/SHP signaling on hepatic XBP1s expression, we administered GW4064 (150 mg/kg, 16 hours) to wild-type mice. Hepatic XBP1s protein was minimally detected at baseline, but increased in response to GW4064 administration (Figure 8A). Hepatic *Xbp1s* gene expression also increased in response to GW4064 (Figure 8B). Hepatic *Xbp1u* gene expression did not alter after GW4064 treatment (Supporting Figure S5). We also examined baseline expression of hepatic *Xbp1s* gene expression in FXR (−/−) and SHP (−/−) mice. Hepatic gene expression of *Xbp1s* was reduced by 52% in FXR (−/−) mice and 45% in SHP (−/−) mice compared to wild-type mice (Figure 8C, 8D). Since baseline hepatic XBP1s protein expression was not detected, reductions cannot be observed.

Discussion

Bile acids are endogenous FXR ligands and hepatic FXR signaling regulates many liver metabolic, transport and injury pathways (28, 29). The high affinity FXR agonist 6-ECDCA has hepatoprotective effects including reduction in inflammation and fibrosis, improving biliary transport, regulating hepatic glucose and lipid metabolism and regulating anti-apoptotic pathways (30–33). 6-ECDCA has been approved for the treatment of Primary Biliary Cholangitis and is currently being studied in clinical trials for other cholestatic, genetic and metabolic liver diseases. However, interactions of bile acid and pharmacologic FXR signaling on activation of the IRE1α/XBP1 pathways remain unexplored. In fact, there are few data demonstrating nuclear receptor regulation of any UPR pathways.

We demonstrate that activating FXR signaling by bile acids or FXR agonists induces XBP1s expression *in vivo* and *in vitro*. Mice fed a diet enriched in the FXR bile acid agonist DCA have increased hepatic expression of XBP1s and its downstream target ERdj4. These changes occur concomitantly with increases of bile acid pool and content of the FXR bile acid ligands TCDCA, TCA and TDCA. After one day of DCA feeding, there was no histologic or biochemical evidence of liver injury, suggesting that the early activation of the XBP1s pathway may be due to factors other than liver injury. In fact, the gene expression of other UPR pathways remained unchanged or decreased at all time points studied. Previous data demonstrated that mice fed 0.5% cholic acid for a week have a nine-fold increase in hepatic *Xbp1s*, although the UPR genes *Atf6* and *Chop* also increased (24). Differences in gene expression may be due to their use of a higher dose of a different bile acid and/or difference in mouse strain background. The hydrophobic bile acid DCA has been demonstrated to causes protein unfolding and aggregation *in vitro* (11), therefore, we do not exclude the possibility that other UPR pathways can be activated with DCA feeding at other time points or doses. Of note, the hydrophilic bile acid TUDCA can act as a chemical chaperone and potentially reduce ER stress (34). In addition, we also demonstrated the hepatic XBP1s expression similarly increases in a bile duct ligation model of cholestasis.

We fed mice cholestyramine for 7 days to diminish the bile acid pool. Cholestyramine is a relatively inert bile acid binding resin that is not absorbed, so it is unlikely to cause hepatic ER stress or liver injury. Baseline gene expression of hepatic *Ire1α*, *Xbp1s* and *Xbp1u* all decrease with cholestyramine feeding, although *ERdj4* remains unchanged. *ERdj4* is also regulated by IRE1α-independent pathways that may account for this lack of suppression (35). In contrast to the IRE1α/XBP1 pathway, hepatic expression of the UPR genes *Atf4*, *Atf6*, *Bip* and *Chop* are not reduced. We subsequently treated Huh7-Ntcp cells with several bile acids and detected *in vitro* activation of the IRE1α/XBP1 pathway, similar to that observed *in vivo*. These effects occur at a lower bile acid concentration than those often used for *in vitro* bile acid toxicity studies (20, 36, 37).

To further determine that these effects are mediated, at least in part, by FXR signaling, we used two distinct high-affinity FXR agonists (6-ECDCA and GW4064) and two different liver cell lines (HepG2, Huh7-Ntcp) to demonstrate that IRE1α/XBP1 pathway was activated in a dose-dependent manner. FXR agonists have multiple hepatoprotective effects and it is unlikely the FXR agonists induce ER stress. This further supports that the IRE1α/XBP1 pathway activation is FXR-mediated, rather than secondary to generalized ER stress. We next determined that both basal and FXR agonists-induced expression of XBP1s protein is blocked by the FXR antagonist guggulsterone and by FXR-knockdown, further demonstrating the specificity of FXR regulation.

The major regulation of the IRE1α/XBP1 pathway is via the atypical splicing of the unspliced form of *XBP1* to *XBP1s* by p-IRE1α. We employed a luciferase reporter construct to demonstrate that FXR agonists increase XBP1 splicing. The endoribonuclease activity of p-IRE1α is the only enzymatic activity known to splice XBP1 and therefore the luciferase reporter construct is specific for p-IRE1α splicing of XBP1 (38, 39). We demonstrated that FXR agonists simultaneously increase p-IRE1α expression, providing a putative mechanism for the increased splicing activity. Many FXR functions are mediated by SHP and both FXR

agonists induce *SHP* mRNA expression, preceding IRE1α phosphorylation. We demonstrated the role of SHP in activating p-IRE1α and XBP1s by SHP overexpression and knockdown experiments. Unfortunately, we were unable to detect increased p-IRE1α expression in our *in vivo* models, probably due to low level of expression at the time points studied. We cannot exclude the possibility that p-IRE1α was increased at other time points or that XBP1s was regulated through other mechanisms in addition to p-IRE1α activation. The hepatic gene expression of XBP1u didn't change after GW4064 treatment in mice. Analysis of genome-wide chromatin immunoprecipitation-sequencing (ChIP-Seq) of FXR binding data shows potentially weak binding of FXR to the XBP1 immediate promoter region and at the junction of second exon-intron (40), although the physiological significance remains to be determined. We cannot exclude that possibility of additional transcriptional regulation of XBP1 by FXR.

Recent studies have shown that IRE1α signaling can be regulated independent of ER stress through protein interactions (23). Although SHP is generally considered as a transcriptional repressor, it has now been shown to interact with other proteins and regulate functions throughout the cell (27, 41–43). We demonstrate that SHP and IRE1α can interact and this interaction may be responsible for the increased p-IRE1α and XBP1s expression that occurs with FXR agonist stimulation. FXR shares many common target genes with LRH-1. A recent study has shown that nuclear receptor LRH-1 initiates an ER stress resolution pathway by inducing PLK3 expression, which phosphorylates ATF2 (44). We did not observe any change in *PLK3* gene expression with FXR agonist treatment, although regulation could also be post-transcriptional.

FXR agonists and FXR-mediated IRE1α/XBP1 pathway activation may be particularly beneficial during pathologic states of cholestasis when bile acid concentrations increase. Pharmacologic FXR agonists have beneficial anti-inflammatory, anti-cholestatic and anti-fibrotic effects on the liver; as well as beneficial effects on glucose and lipid metabolism (45, 46). Our data demonstrate that FXR agonists may also be hepatoprotective due to the previously unidentified interaction with the IRE1α/XBP1 pathway. However, we do not exclude the possible involvement of the PERK and ATF6 pathways.

The pathogenesis of primary biliary cholangitis (PBC) has been associated with ER stress (47) and a recent clinical trial demonstrated that obeticholic acid (6-ECDCA) is beneficial in patients with PBC who had inadequate responses to ursodeoxycholic acid (48). Dysregulation of XBP1 has also been shown to be important in the pathogenesis of nonalcoholic steatohepatitis (NASH) (49) and obeticholic acid may improve liver histology in patients with non-cirrhotic NASH (50). The pathogenesis of PBC and NASH are multi-factorial and FXR-mediated activation of the IRE1α/XBP1 pathway provides a novel pathway for targeting new treatments of these and other forms of liver diseases.

Many hepatic diseases cause ER stress and the unfolded protein response is an essential compensatory mechanism to resolve ER stress in the liver. We now demonstrate that FXR signaling activates the IRE1α/XBP1 pathway in the liver, at least in part, via SHP signaling. These data will enhance our understanding of IRE1α/XBP1 pathway regulation in both normal and pathologic states in the liver and may have important therapeutic implications.

Supplementary Material

Refer to Web version on PubMed Central for supplementary material.

Acknowledgments

List of Abbreviations

UPR	unfolded protein response
ER	endoplasmic reticulum
IRE1α	inositol-requiring enzyme 1α
PERK	PKR-like ER kinase
ATF4/6	activating transcription factor 4/6
XBP1	X-box binding protein 1
ERAD	endoplasmic reticulum-associated protein degradation
DCA	deoxycholic acid
FXR	farnesoid X receptor
SHP	small heterodimer partner
GAPDH	glyceraldehyde 3-phosphate dehydrogenase
ALT	alanine aminotransferase
NTCP	sodium-taurocholate polypeptide
TCA	taurocholic acid
TDCA	taurodeoxycholic acid
TCDCA	taurochenodeoxycholic acid
TMCA	tauromuricholic acid
6-ECDCA	6α-ethyl-chenodeoxycholic acid
ERdj4/DNAJB9	DnaJ (Hsp40) homolog, subfamily B, member 9/ endoplasmic reticulum DNA J domain-containing protein 4

BIP/GRP78	binding immunoglobulin protein/glucose-regulated protein, 78 kDa
CHOP	C/EBP-homologous protein
PLK3	polo-like kinase 3

References

1. Wu J, Kaufman RJ. From acute ER stress to physiological roles of the Unfolded Protein Response. Cell Death Differ. 2006; 13:374–384. [PubMed: 16397578]

2. Marciniak SJ, Ron D. Endoplasmic reticulum stress signaling in disease. Physiol Rev. 2006; 86:1133–1149. [PubMed: 17015486]

3. Kaufman RJ. Stress signaling from the lumen of the endoplasmic reticulum: coordination of gene transcriptional and translational controls. Genes Dev. 1999; 13:1211–1233. [PubMed: 10346810]

4. Malhi H, Kaufman RJ. Endoplasmic reticulum stress in liver disease. J Hepatol. 2011; 54:795–809. [PubMed: 21145844]

5. Lee AH, Iwakoshi NN, Glimcher LH. XBP-1 regulates a subset of endoplasmic reticulum resident chaperone genes in the unfolded protein response. Mol Cell Biol. 2003; 23:7448–7459. [PubMed: 14559994]

6. Hetz C, Martinon F, Rodriguez D, Glimcher LH. The unfolded protein response: integrating stress signals through the stress sensor IRE1alpha. Physiol Rev. 2011; 91:1219–1243. [PubMed: 22013210]

7. Liu X, Henkel AS, LeCuyer BE, Schipma MJ, Anderson KA, Green RM. Hepatocyte X-box binding protein 1 deficiency increases liver injury in mice fed a high-fat/sugar diet. Am J Physiol Gastrointest Liver Physiol. 2015; 309:G965–974. [PubMed: 26472223]

8. Lee J, Ozcan U. Unfolded protein response signaling and metabolic diseases. J Biol Chem. 2014; 289:1203–1211. [PubMed: 24324257]

9. Hur KY, So JS, Ruda V, Frank-Kamenetsky M, Fitzgerald K, Koteliansky V, Iwawaki T, et al. IRE1alpha activation protects mice against acetaminophen-induced hepatotoxicity. J Exp Med. 2012; 209:307–318. [PubMed: 22291093]

10. Cremers CM, Knoefler D, Vitvitsky V, Banerjee R, Jakob U. Bile salts act as effective protein-unfolding agents and instigators of disulfide stress in vivo. Proc Natl Acad Sci U S A. 2014; 111:E1610–1619. [PubMed: 24706920]

11. Wang H, Chen J, Hollister K, Sowers LC, Forman BM. Endogenous bile acids are ligands for the nuclear receptor FXR/BAR. Mol Cell. 1999; 3:543–553. [PubMed: 10360171]

12. Parks DJ, Blanchard SG, Bledsoe RK, Chandra G, Consler TG, Kliewer SA, Stimmel JB, et al. Bile acids: natural ligands for an orphan nuclear receptor. Science. 1999; 284:1365–1368. [PubMed: 10334993]

13. Zhang Y, Hagedorn CH, Wang L. Role of nuclear receptor SHP in metabolism and cancer. Biochim Biophys Acta. 2011; 1812:893–908. [PubMed: 20970497]

14. Zhan L, Liu HX, Fang Y, Kong B, He Y, Zhong XB, Fang J, et al. Genome-wide binding and transcriptome analysis of human farnesoid X receptor in primary human hepatocytes. PLoS One. 2014; 9:e105930. [PubMed: 25198545]

15. Wang YD, Chen WD, Moore DD, Huang W. FXR: a metabolic regulator and cell protector. Cell Res. 2008; 18:1087–1095. [PubMed: 18825165]

16. Lefebvre P, Cariou B, Lien F, Kuipers F, Staels B. Role of bile acids and bile acid receptors in metabolic regulation. Physiol Rev. 2009; 89:147–191. [PubMed: 19126757]

17. Yang Z, Tsuchiya H, Zhang Y, Lee S, Liu C, Huang Y, Vargas GM, et al. REV-ERBalpha Activates C/EBP Homologous Protein to Control Small Heterodimer Partner-Mediated Oscillation of Alcoholic Fatty Liver. Am J Pathol. 2016; 186:2909–2920. [PubMed: 27664470]

18. Kong B, Wang L, Chiang JY, Zhang Y, Klaassen CD, Guo GL. Mechanism of tissue-specific farnesoid X receptor in suppressing the expression of genes in bile-acid synthesis in mice. Hepatology. 2012; 56:1034–1043. [PubMed: 22467244]

19. Henkel AS, Anderson KA, Dewey AM, Kavesh MH, Green RM. A chronic high-cholesterol diet paradoxically suppresses hepatic CYP7A1 expression in FVB/NJ mice. J Lipid Res. 2011; 52:289–298. [PubMed: 21097822]

20. Rust C, Wild N, Bernt C, Vennegeerts T, Wimmer R, Beuers U. Bile acid-induced apoptosis in hepatocytes is caspase-6-dependent. J Biol Chem. 2009; 284:2908–2916. [PubMed: 19017654]

21. Spiotto MT, Banh A, Papandreou I, Cao H, Galvez MG, Gurtner GC, Denko NC, et al. Imaging the unfolded protein response in primary tumors reveals microenvironments with metabolic variations that predict tumor growth. Cancer Res. 2010; 70:78–88. [PubMed: 20028872]

22. Zhou T, Zhang Y, Macchiarulo A, Yang Z, Cellanetti M, Coto E, Xu P, et al. Novel polymorphisms of nuclear receptor SHP associated with functional and structural changes. J Biol Chem. 2010; 285:24871–24881. [PubMed: 20516075]

23. Qiu Q, Zheng Z, Chang L, Zhao YS, Tan C, Dandekar A, Zhang Z, et al. Toll-like receptor-mediated IRE1alpha activation as a therapeutic target for inflammatory arthritis. EMBO J. 2013; 32:2477–2490. [PubMed: 23942232]

24. Bochkis IM, Rubins NE, White P, Furth EE, Friedman JR, Kaestner KH. Hepatocyte-specific ablation of Foxa2 alters bile acid homeostasis and results in endoplasmic reticulum stress. Nat Med. 2008; 14:828–836. [PubMed: 18660816]

25. Calfon M, Zeng H, Urano F, Till JH, Hubbard SR, Harding HP, Clark SG, et al. IRE1 couples endoplasmic reticulum load to secretory capacity by processing the XBP-1 mRNA. Nature. 2002; 415:92–96. [PubMed: 11780124]

26. Zhang Y, Soto J, Park K, Viswanath G, Kuwada S, Abel ED, Wang L. Nuclear receptor SHP, a death receptor that targets mitochondria, induces apoptosis and inhibits tumor growth. Mol Cell Biol. 2010; 30:1341–1356. [PubMed: 20065042]

27. Zhang Y, Wang L. Characterization of the mitochondrial localization of the nuclear receptor SHP and regulation of its subcellular distribution by interaction with Bcl2 and HNF4alpha. PLoS One. 2013; 8:e68491. [PubMed: 23874642]

28. Houten SM, Watanabe M, Auwerx J. Endocrine functions of bile acids. EMBO J. 2006; 25:1419–1425. [PubMed: 16541101]

29. Huang W, Ma K, Zhang J, Qatanani M, Cuvillier J, Liu J, Dong B, et al. Nuclear receptor-dependent bile acid signaling is required for normal liver regeneration. Science. 2006; 312:233–236. [PubMed: 16614213]

30. Ghebremariam YT, Yamada K, Lee JC, Johnson CL, Atzler D, Anderssohn M, Agrawal R, et al. FXR agonist INT-747 upregulates DDAH expression and enhances insulin sensitivity in high-salt fed Dahl rats. PLoS One. 2013; 8:e60653. [PubMed: 23593273]

31. Hollman DA, Milona A, van Erpecum KJ, van Mil SW. Anti-inflammatory and metabolic actions of FXR: insights into molecular mechanisms. Biochim Biophys Acta. 2012; 1821:1443–1452. [PubMed: 22820415]

32. Pellicciari R, Fiorucci S, Camaioni E, Clerici C, Costantino G, Maloney PR, Morelli A, et al. 6alpha-ethyl-chenodeoxycholic acid (6-ECDCA), a potent and selective FXR agonist endowed with anticholestatic activity. J Med Chem. 2002; 45:3569–3572. [PubMed: 12166927]

33. Fiorucci S, Antonelli E, Rizzo G, Renga B, Mencarelli A, Riccardi L, Orlandi S, et al. The nuclear receptor SHP mediates inhibition of hepatic stellate cells by FXR and protects against liver fibrosis. Gastroenterology. 2004; 127:1497–1512. [PubMed: 15521018]

34. Ozcan U, Yilmaz E, Ozcan L, Furuhashi M, Vaillancourt E, Smith RO, Gorgun CZ, et al. Chemical chaperones reduce ER stress and restore glucose homeostasis in a mouse model of type 2 diabetes. Science. 2006; 313:1137–1140. [PubMed: 16931765]

35. Hollien J, Lin JH, Li H, Stevens N, Walter P, Weissman JS. Regulated Ire1-dependent decay of messenger RNAs in mammalian cells. J Cell Biol. 2009; 186:323–331. [PubMed: 19651891]

36. Faubion WA, Guicciardi ME, Miyoshi H, Bronk SF, Roberts PJ, Svingen PA, Kaufmann SH, et al. Toxic bile salts induce rodent hepatocyte apoptosis via direct activation of Fas. J Clin Invest. 1999; 103:137–145. [PubMed: 9884343]

37. Granato A, Gores G, Vilei MT, Tolando R, Ferraresso C, Muraca M. Bilirubin inhibits bile acid induced apoptosis in rat hepatocytes. Gut. 2003; 52:1774–1778. [PubMed: 14633961]

38. Prischi F, Nowak PR, Carrara M, Ali MM. Phosphoregulation of Ire1 RNase splicing activity. Nat Commun. 2014; 5:3554. [PubMed: 24704861]

39. Ali MM, Bagratuni T, Davenport EL, Nowak PR, Silva-Santisteban MC, Hardcastle A, McAndrews C, et al. Structure of the Ire1 autophosphorylation complex and implications for the unfolded protein response. EMBO J. 2011; 30:894–905. [PubMed: 21317875]

40. Thomas AM, Hart SN, Kong B, Fang J, Zhong XB, Guo GL. Genome-wide tissue-specific farnesoid X receptor binding in mouse liver and intestine. Hepatology. 2010; 51:1410–1419. [PubMed: 20091679]

41. Yang CS, Kim JJ, Kim TS, Lee PY, Kim SY, Lee HM, Shin DM, et al. Small heterodimer partner interacts with NLRP3 and negatively regulates activation of the NLRP3 inflammasome. Nat Commun. 2015; 6:6115. [PubMed: 25655831]

42. Yuk JM, Shin DM, Lee HM, Kim JJ, Kim SW, Jin HS, Yang CS, et al. The orphan nuclear receptor SHP acts as a negative regulator in inflammatory signaling triggered by Toll-like receptors. Nat Immunol. 2011; 12:742–751. [PubMed: 21725320]

43. Kim YC, Byun S, Zhang Y, Seok S, Kemper B, Ma J, Kemper JK. Liver ChIP-seq analysis in FGF19-treated mice reveals SHP as a global transcriptional partner of SREBP-2. Genome Biol. 2015; 16:268. [PubMed: 26634251]

44. Mamrosh JL, Lee JM, Wagner M, Stambrook PJ, Whitby RJ, Sifers RN, Wu SP, et al. Nuclear receptor LRH-1/NR5A2 is required and targetable for liver endoplasmic reticulum stress resolution. Elife. 2014; 3:e01694. [PubMed: 24737860]

45. Wang YD, Chen WD, Wang M, Yu D, Forman BM, Huang W. Farnesoid X receptor antagonizes nuclear factor kappaB in hepatic inflammatory response. Hepatology. 2008; 48:1632–1643. [PubMed: 18972444]

46. Verbeke L, Farre R, Trebicka J, Komuta M, Roskams T, Klein S, Elst IV, et al. Obeticholic acid, a farnesoid X receptor agonist, improves portal hypertension by two distinct pathways in cirrhotic rats. Hepatology. 2014; 59:2286–2298. [PubMed: 24259407]

47. Sasaki M, Yoshimura-Miyakoshi M, Sato Y, Nakanuma Y. A possible involvement of endoplasmic reticulum stress in biliary epithelial autophagy and senescence in primary biliary cirrhosis. J Gastroenterol. 2015; 50:984–995. [PubMed: 25552342]

48. Hirschfield GM, Mason A, Luketic V, Lindor K, Gordon SC, Mayo M, Kowdley KV, et al. Efficacy of obeticholic acid in patients with primary biliary cirrhosis and inadequate response to ursodeoxycholic acid. Gastroenterology. 2015; 148:751–761 e758. [PubMed: 25500425]

49. Puri P, Mirshahi F, Cheung O, Natarajan R, Maher JW, Kellum JM, Sanyal AJ. Activation and dysregulation of the unfolded protein response in nonalcoholic fatty liver disease. Gastroenterology. 2008; 134:568–576. [PubMed: 18082745]

50. Neuschwander-Tetri BA, Loomba R, Sanyal AJ, Lavine JE, Van Natta ML, Abdelmalek MF, Chalasani N, et al. Farnesoid X nuclear receptor ligand obeticholic acid for non-cirrhotic, non-alcoholic steatohepatitis (FLINT): a multicentre, randomised, placebo-controlled trial. Lancet. 2015; 385:956–965. [PubMed: 25468160]
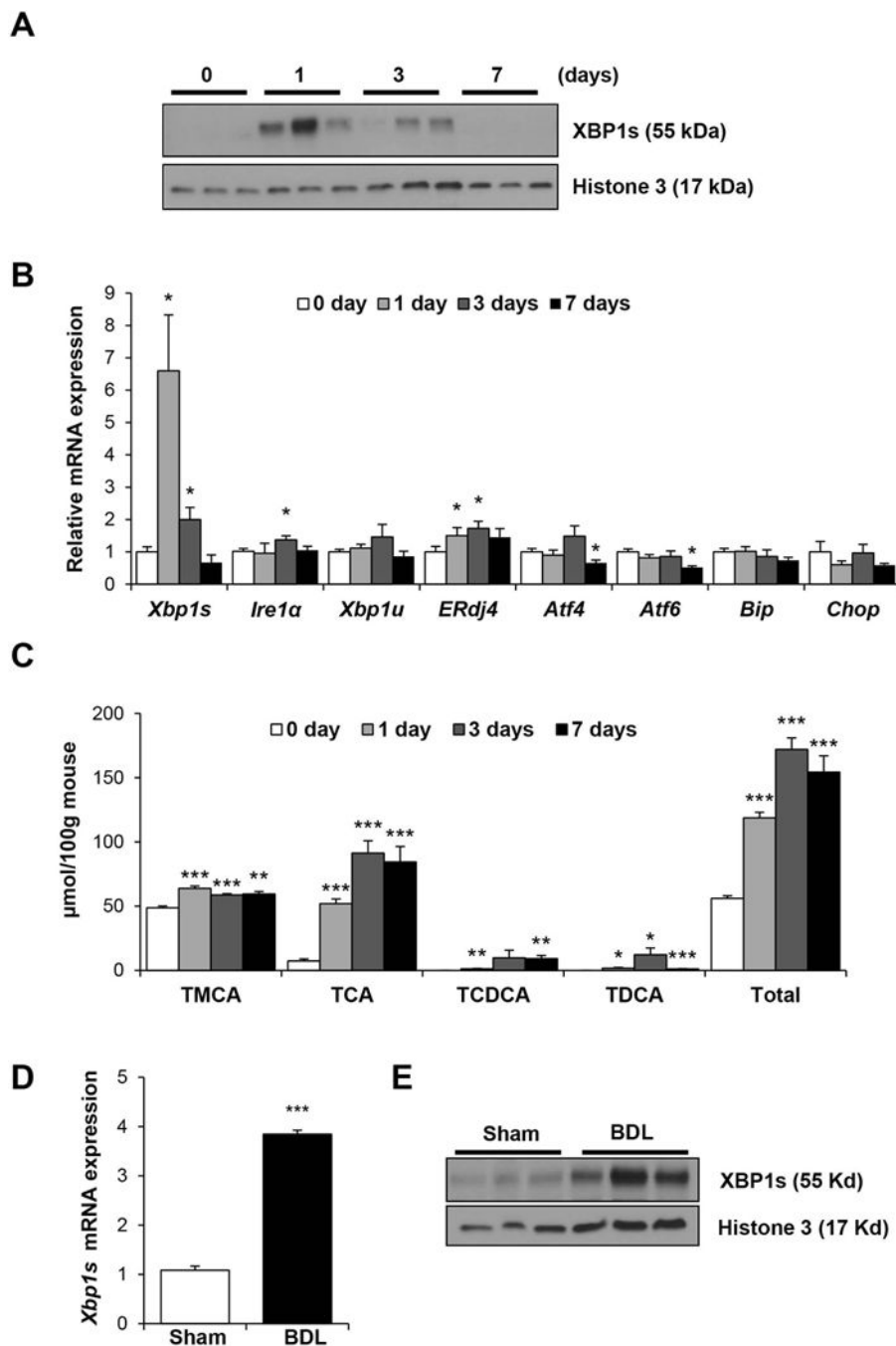
Figure 1. Hepatic UPR gene expression and bile acid pool in mice fed deoxycholic acid (DCA) and subjected to bile duct ligation (BDL)

Male FVB/NJ mice were fed chow supplemented with 0.3% DCA for 1, 3 and 7 days or chow-alone (0 day) (n=5). A) Western blot of hepatic nuclear XBP1s is shown with histone 3 used as a loading control. B) Hepatic gene expression was measured using qPCR. DCA-fed mice have increased hepatic gene expression of *Xbp1s*, *ERdj4*, and *Ire1α*. C) Bile acid composition and total bile acid pool in DCA- and chow-fed mice. D) Female C57BL/6J mice were subjected to BDL or sham operation (n=3) for 48 hours. Hepatic *Xbp1s* mRNA was measured by qPCR. E) Western blot of hepatic nuclear XBP1s is shown with histone 3

used as a loading control. *P< 0.05, **P< 0.01, ***P< 0.001 compared to 0 day or sham-control.
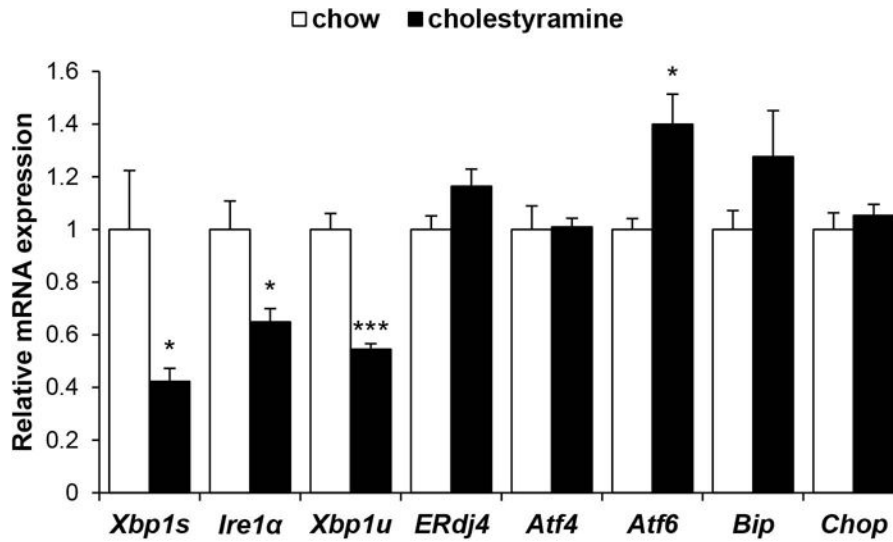
Figure 2. Hepatic UPR pathway gene expression in mice fed cholestyramine
Male FVB/NJ mice were fed chow with 2% cholestyramine or chow-alone for 7 days and hepatic gene expression was measured using qPCR (n=5). Cholestyramine feeding decreases basal gene expression of *Xbp1s*, *Xbp1u* and *Ire1a*. *$P < 0.05$, ***$P < 0.001$ compared to chow.
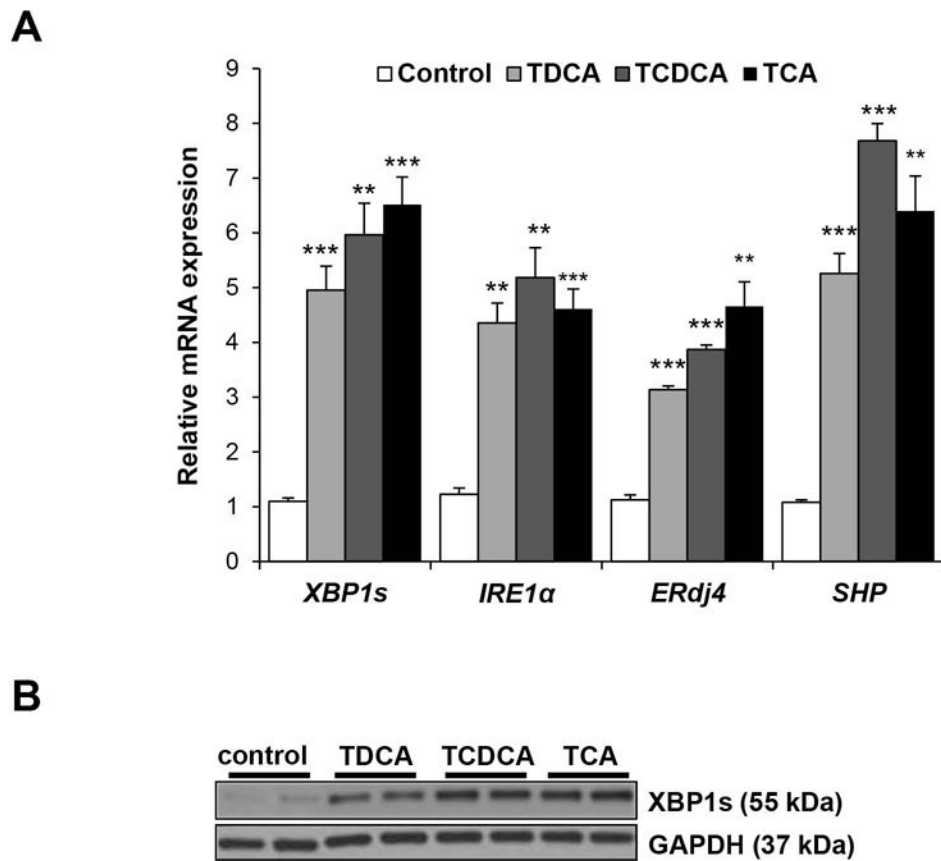
A

B

Figure 3. XBP1s protein and gene expression of Huh7-Ntcp cells treated with bile acids
Huh7-Ntcp cells were treated with TCA (10 μM), TDCA (10 μM) and TCDCA (10 μM) for 6 hours. A) *XBP1s*, *ERdj4, IRE1α* and *SHP* gene expression was measured using qPCR. B) XBP1s protein expression was examined in cell homogenate using western blotting with GAPDH used as a loading control. $**P < 0.01$, $***P < 0.001$ compared to control.
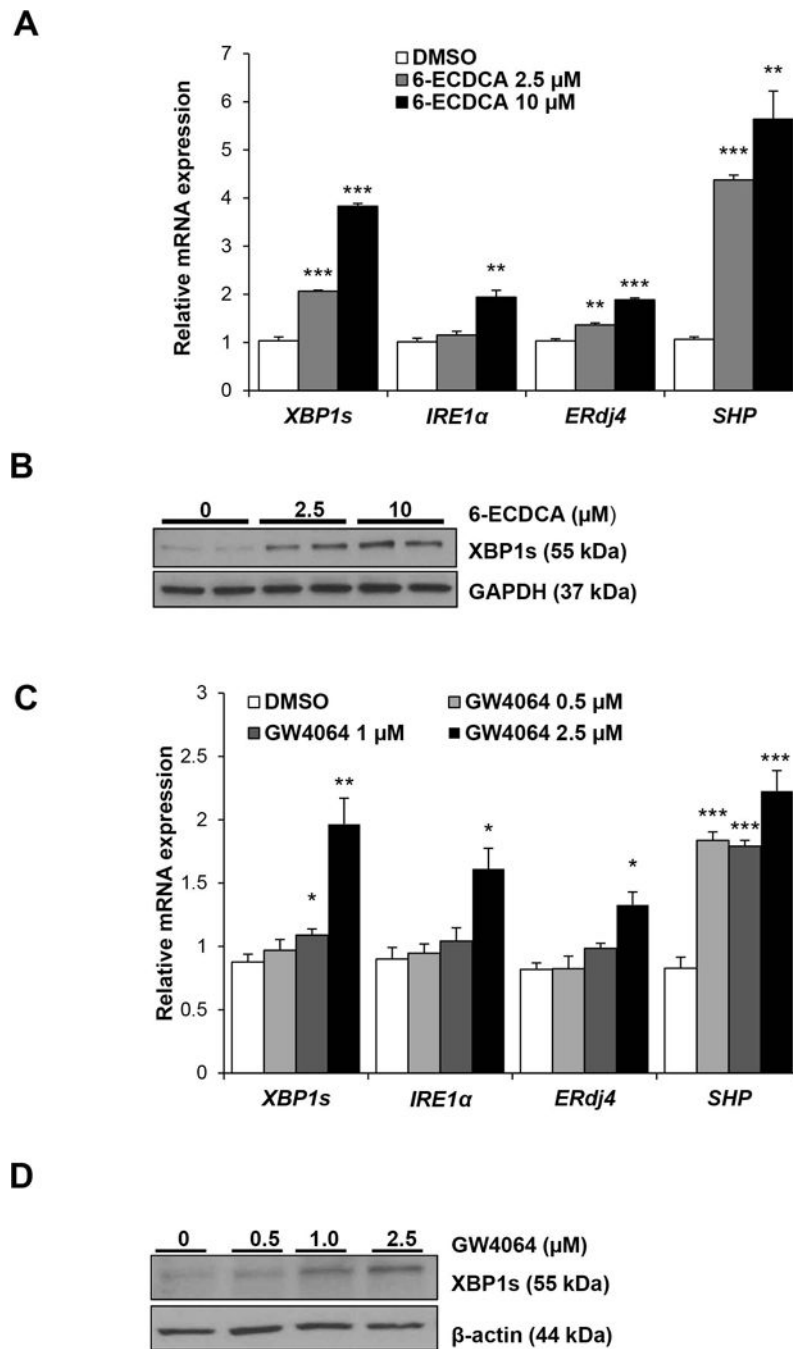
Figure 4. XBP1s protein and gene expression of Huh7-Ntcp and HepG2 cells treated with FXR agonists

A) Huh7-Ntcp cells were treated with 6-ECDCA (0-10 μM) or DMSO vehicle for 4 hours and *IRE1α*, *XBP1s*, *ERdj4* and *SHP* gene expression was measured with qPCR. B) Representative western blot of XBP1s is shown with GAPDH used as a loading control. C) HepG2 cells were treated with GW4064 (0-2.5 μM) or DMSO vehicle for 6 hours and *IRE1α*, *XBP1s*, *ERdj4* and *SHP* gene expression was measured. D) Representative western blot of XBP1s is shown with β-actin used as a loading control. $*P < 0.05$, $**P < 0.01$, $***P < 0.001$ compared to DMSO.

A

B
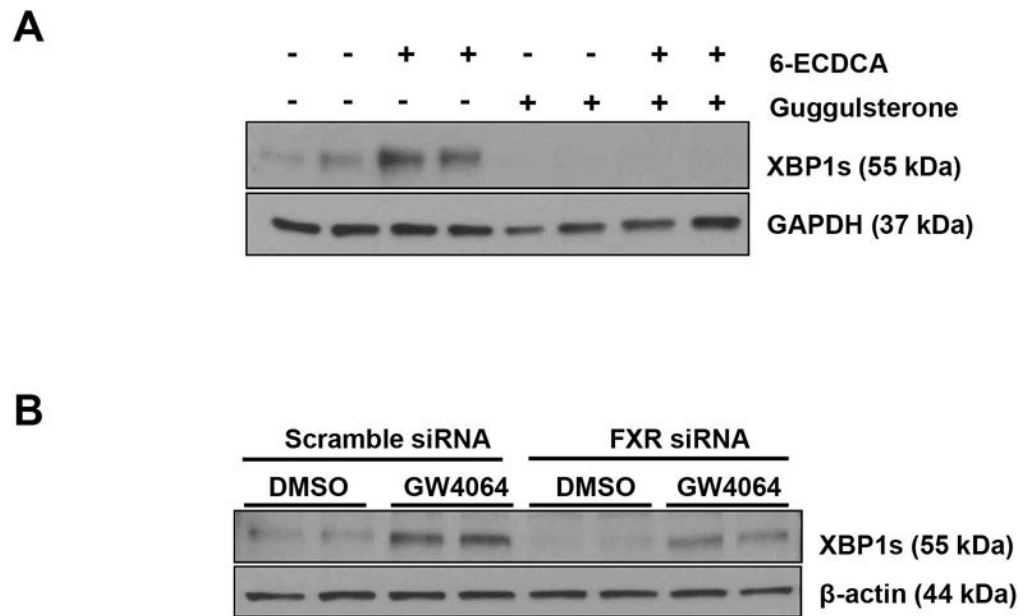
Figure 5. Guggulsterone and FXR siRNA reduce XBP1s protein expression

A) Huh7-Ntcp cells were pre-treated with 50 μM guggulsterone for 1 hour prior to 8 hours of treatment with 6-ECDCA (10 μM) or DMSO vehicle. Representative western blot of XBP1s is shown with GAPDH used as a loading control. Basal XBP1s and 6-ECDCA-induced XBP1s protein expression are both reduced by guggulsterone treatment. B) HepG2 cells were transfected with either FXR siRNA or scramble siRNA and subsequently treated with 2.5 μM of GW4064 or DMSO vehicle for 6 hours. Representative western blot of XBP1s is shown with β-actin used as a loading control. Basal XBP1s and GW4064-induced XBP1s protein expression are both reduced by FXR siRNA.
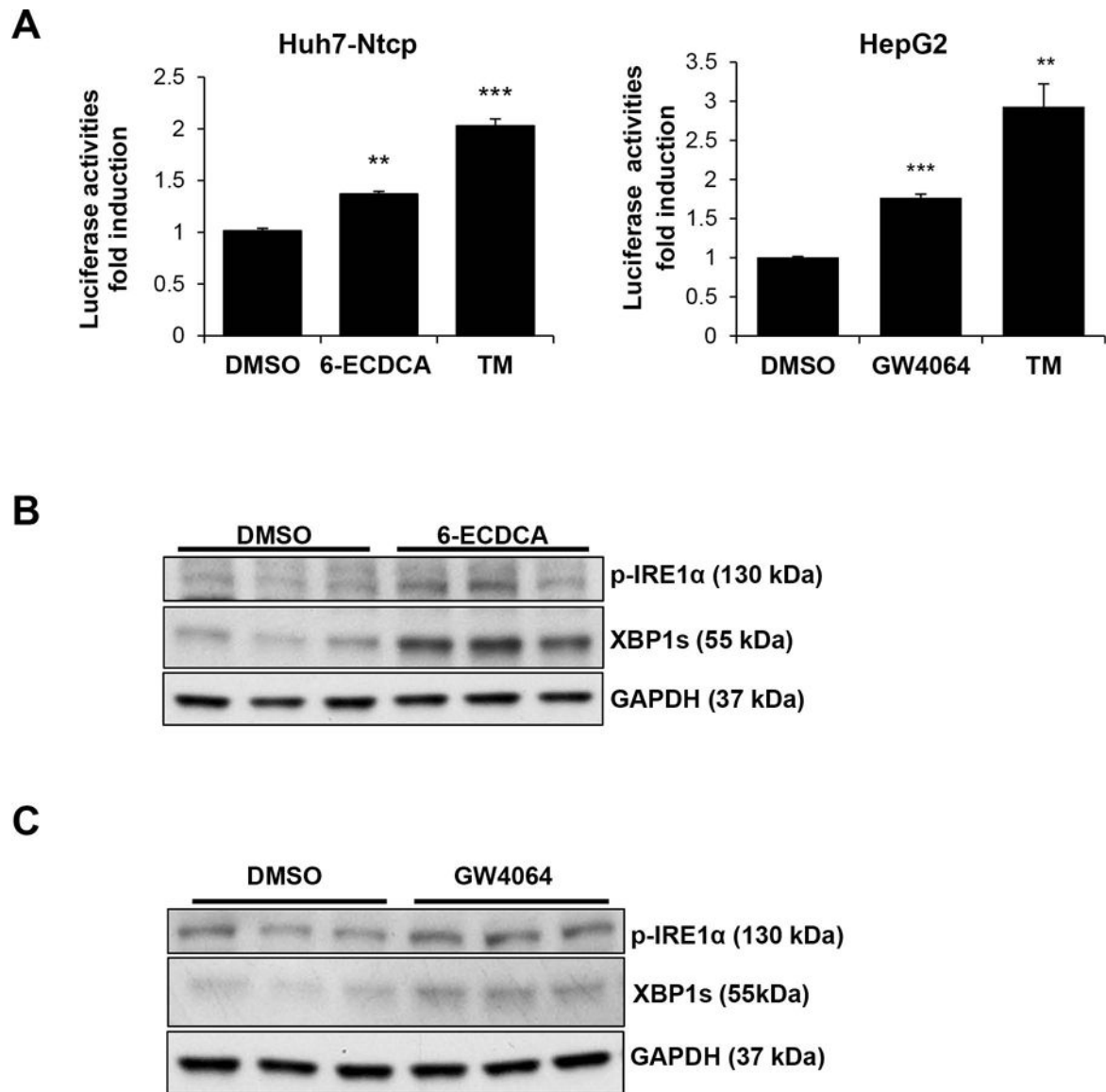
Figure 6. FXR agonists increase XBP1 splicing and IRE1α phosphorylation
A) Huh7-Ntcp and HepG2 cells were transfected with an XBP1 splicing activity-luciferase reporter gene (XBP1-luc) and treated with 10 μM 6-ECDCA or 2.5 μM GW4064, respectively for 8 hours. The splicing of XBP1 was measured by luciferase assay. Tunicamycin (TM, 2.5 μg/ml) was used as a positive control for XBP1 splicing. $**P < 0.01$, $***P < 0.001$ compared to DMSO. B) Huh7-Ntcp cells were treated with 2.5 μM 6-ECDCA or DMSO for 2 hours, and C) HepG2 cells were treated with 2.5 μM GW4064 or DMSO for 4 hours. Western blotting was performed for phosphorylated-IRE1α (p-IRE1α). Cellular p-IRE1α expression is increased in Huh7-Ntcp and HepG2 cells in response to FXR-agonist treatment. XBP1s and GAPDH protein expression are also shown.
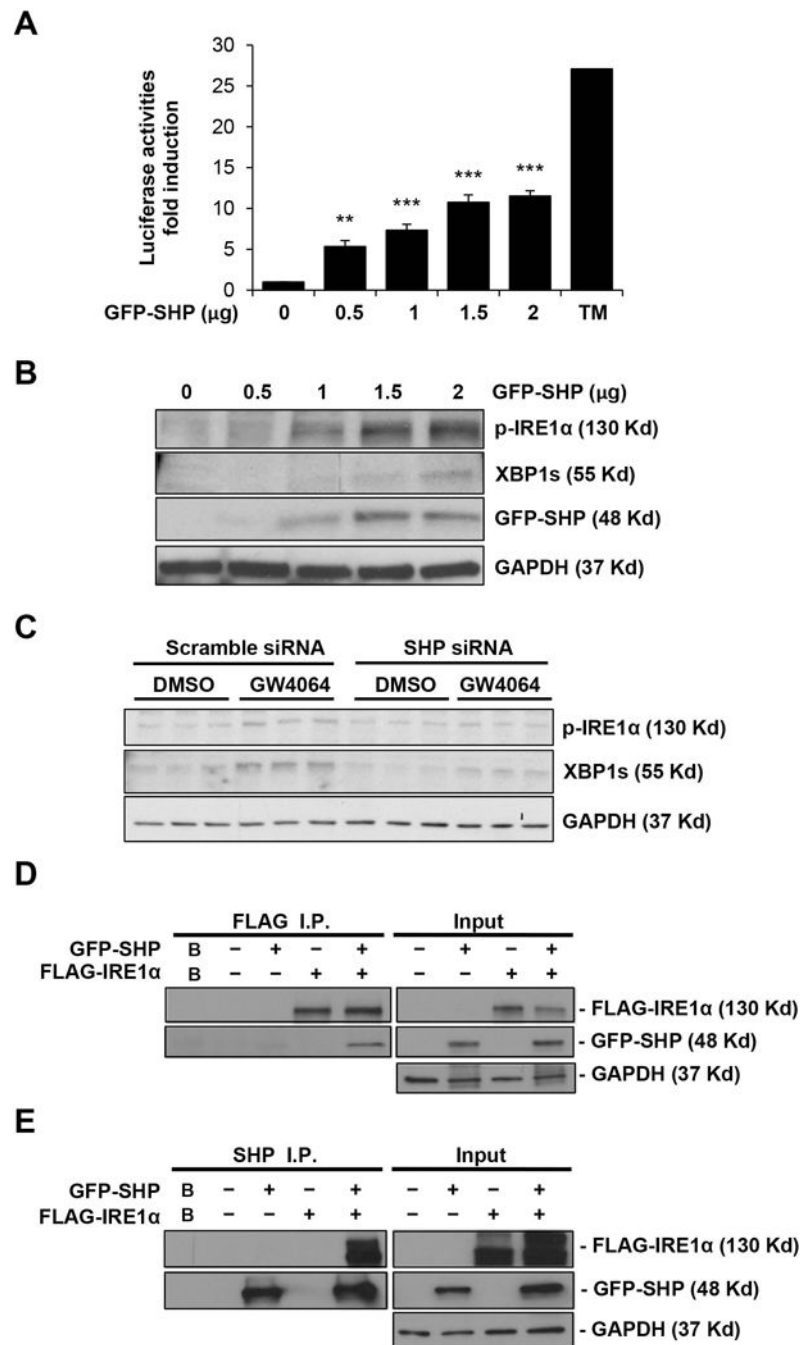
Figure 7. SHP is associated with increased XBP1 splicing and IRE1α phosphorylation, and interacts with IRE1α

A) HepG2 cells were co-transfected with the XBP1-luc reporter gene and either pcDNA vector or GFP-SHP expression plasmid (0-2 μg) for 48 hours. The splicing of XBP1 was measured by luciferase assay (n=3). Tunicamycin treatment (10 μM, 48 hours, n= 2) was used as a positive control. **P< 0.01, ***P< 0.001 compared to pcDNA alone-transfected cells. B) HepG2 cells were transfected with GFP-SHP expression plasmid (0-2 μg). Representative western blots of p-IRE1α, XBP1s, GFP-SHP are shown with GAPDH as a loading control. C) HepG2 cells were transfected with either SHP siRNA or scramble

siRNA and subsequently treated with 2.5 μM of GW4064 or DMSO vehicle for 6 hours. Representative western blots of p-IRE1α and XBP1s are shown with GAPDH used as a loading control. Basal XBP1s and GW4064-induced XBP1s protein expression are both reduced by SHP siRNA. D, E) HEK293T cells were transfected with indicated plasmids and immunoprecipitated with anti-FLAG or anti-SHP antibody. Immunoprecipitates and 5% inputs were subjected to SDS-PAGE and probed with indicated antibodies. pcDNA3 vector-alone was included to ensure equal amount of total DNA in each transfection. B: buffer only as negative control.
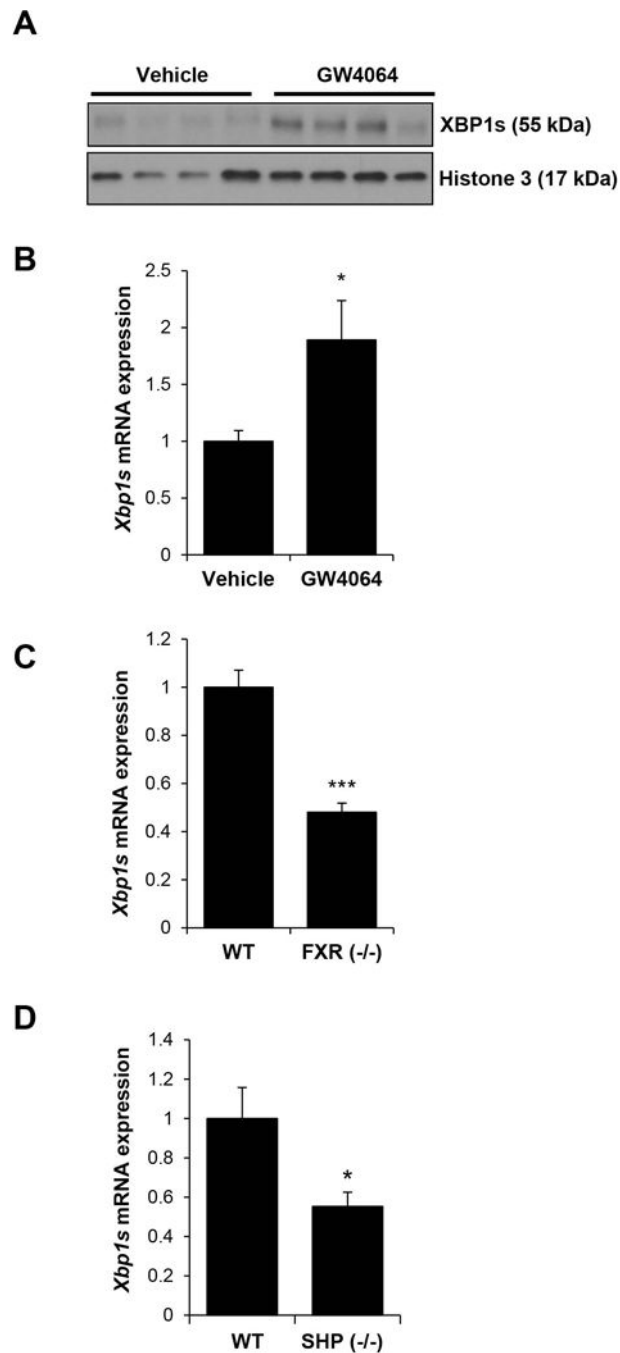
Figure 8. FXR/SHP signaling regulates XBP1s expression in vivo

A) Male C57BL/6J mice were administered with either vehicle or GW4064 (150 mg/kg) and livers harvested after 16 hours. Nuclear content of XBP1s was measured by western blot with histone 3 as a loading control. B) Hepatic *Xbp1s* mRNA level was measured with qPCR in vehicle- or GW4064-treated mice. *$P < 0.05$ compared to vehicle-treated mice. C) Hepatic *Xbp1s* mRNA level was measured with qPCR in wild-type (WT) or FXR (−/−)

mice. ***$P < 0.001$ compared to WT mice. D) Hepatic *Xbp1s* mRNA level was measured in WT or SHP (−/−) mice. *$P < 0.05$ compared to WT mice.